Available online at www.sciencedirect.com
SCIENCE DIRECT®
International Journal of Pharmaceutics 273 (2004) 95–107
international journal of pharmaceutics
www.elsevier.com/locate/ijpharm

All-*trans*-retinoic acid release from core-shell type nanoparticles of poly(ε-caprolactone)/poly (ethylene glycol) diblock copolymer

Young-Il Jeong [a], Myung-Ki Kang [b], Heung-Suk Sun [a], Sam-Suk Kang [b], Hyun-Woo Kim [b], Kyung-Sub Moon [b], Kil-Jung Lee [b], Soo-Han Kim [b], Shin Jung [a,b,c,*]

[a] *Brain Tumor Research Laboratory, Chonnam National University Medical School, Gwangju 501-746, Korea*
[b] *Department of Neurosurgery, Chonnam National University Hospital and Medical School, Gwangju 501-746, Korea*
[c] *Research Institute of Medical Sciences, Chonnam National University Medical School, Gwangju 501-746, Korea*

Received 3 July 2003; received in revised form 12 December 2003; accepted 16 December 2003

Abstract

Poly(ε-caprolactone)/poly(ethylene glycol) (abbreviated as CE) diblock copolymers were synthesized to make core-shell type nanoparticles for all-*trans*-retinoic acid (atRA). Fluorescence spectroscopy showed that critical association concentration (CAC) value decreased at higher MW of CE diblock copolymer. Drug loading characteristics were studied under various experimental conditions. Drug contents and loading efficiency increased as the MW of poly(ε-caprolactone) (PCL) block of CE and initial drug feeding amount increased. Solvent used and preparation method also affected drug contents and loading efficiency. According to ^{1}H NMR using $CDCl_3$ and D_2O, specific peaks of the PCL block and drug appearing in $CDCl_3$, disappeared at D_2O, suggesting hydrophobic core with hydrophilic shell formed in water. atRA release was faster at smaller MW of copolymer and lower drug contents. Nanoparticles prepared in DMF showed faster release rate compared with those prepared in THF or acetone. Cytotoxicity of atRA against U87MG, U251MG and U343MG cell lines were increased by nanoencapsulation while empty nanoparticles of CE diblock copolymer were not significantly affected.

Keywords: All-*trans*-retinoic acid; Core-shell type nanoparticles; Biodegradable; Sustained release

1. Introduction

Core-shell type nanoparticles (Gref et al., 1994; Jeong et al., 1998) or polymer micelles (Kwon et al., 1993, 1995; La et al., 1996) using amphiphilic block copolymers were extensively investigated during last decade due to their surfactant behavior in aqueous environment and their potential as a drug carriers. Since amphiphilic block copolymers have hydrophobic and hydrophilic domains, hydrophobic domains form the inner-core of the core-shell type nanoparticles, which acts as a drug incorporation site for controlled release. Hydrophobic drugs may be physically entrapped within the core by hydrophobic interactions (Kwon et al., 1995; La et al., 1996). Hydrophilic blocks form a hydrated shell which may cloak the hydrophobic core to prevent quick uptake by the reticulo endothelial system (RES) and active clearing organs such

* Corresponding author. Tel.: +82-62-220-6608; fax: +82-62-224-9865.
E-mail address: sjung@chonnam.ac.kr (S. Jung).

0378-5173/$ – see front matter © 2004 Elsevier B.V. All rights reserved.
doi:10.1016/j.ijpharm.2003.12.012

as the liver, spleen, lung, and kidneys. Therefore, a hydrated shell can increase the blood circulation time of nanoparticles. The reported predominant characteristics of this system are reduced toxic side effects of anti-tumor drugs, passive targeting, solubilization of hydrophobic drugs, stable storage of drugs, long blood circulation, and thermal stability. Kataoka's group (Kwon et al., 1993, 1995; La et al., 1996) has extensively investigated polymeric micelles of diblock copolymers based on poly(β-benzyl-L-aspartate) and poly(ethylene oxide) (PEO) as drug carriers of adriamycin (ADR). They reported that enhanced tumor accumulation of ADR encapsulated polymeric micelles with long blood circulation, resulted in effective treatment of solid tumors by micelle-forming block copolymer–adriamycin conjugates (Yokoyama et al., 1990). Gref et al. (1994) reported on core-shell type nanoparticles by poly(lactide)/poly(ethylene glycol) (PEG) block copolymer and PCL–PEG diblock copolymers prepared by a one-step procedure that showed long blood circulation.

It is known that retinoic acid (RA) and its analog, the retinoids, regulate cell behavior during development and play key roles in cell fate determination, cell division, and cell differentiation (Morris-Kay, 1992). RA has been observed to promote neuronal survival, drive astrocytic differentiation, and inhibit differentiation of O2A progenitor cells in the spinal cord (Noll and Miller, 1994). Especially, retinoids and related compounds such as all-*trans*-retinoic acid (atRA) may have therapeutic value in the treatment of human malignant gliomas (Defer et al., 1997) since retinoids strongly inhibit proliferation and migration in primary cultures of human glioblastoma multiforme (Rotan, 1991; Bouterfa et al., 2000), suggesting that atRA is a adequate chemotherapeutic agent to inhibit local invasion of human malignant gliomas. Also, atRA is effective in the treatment of epithelial and hematological malignancies such as breast cancer (Kalmekerian et al., 1994), head and neck cancer (Giannini et al., 1997), ovarian adenocarcinoma (Krupitza et al., 1995), and acute promyelocytic leukemia (APL) (Huang et al., 1988). Although atRA has been proved to be effective against several malignancies in human clinical trials, the cancer relapsed after a brief remission in many patients who were treated with atRA. Furthermore, atRA has poor aqueous solubility (0.21 mM in physiological solution, pH 7.3) (Szuts and Harosi, 1991) and short half-lives in blood (Achkar et al., 1994; Lin et al., 2000; Estey et al., 1996). Especially, it has very short half-lives in the serum and cerebral tissue (below 1 h) although atRA is an attractive anticancer agent for malignant glioma and permeated well into the white matter of rat brain (Le Doze et al., 2000). Retinoid resistance limits its use as a single agent (Muindi et al., 1992).

In this study, we synthesized diblock copolymers composed of PCL and PEG (abbreviated as CE). Core-shell type nanoparticles of CE were prepared to encapsulate atRA. PCL is a non-toxic biodegradable polymer with hydrophobic characteristics. Poly(ethylene glycol), which is a non-immunogenic and non-toxic water-soluble polymer, has the ability to prevent protein adsorption and attack of RES (Lee et al., 1989). There has been extensively investigated on nanoparticles or liposomes formulation for atRA but nanoparticulate formulation of atRA using diblock copolymer has been rarely reported. The particle size, drug loading capacity, and physicochemical properties of atRA-encapsulated core-shell type nanoparticles of CE diblock copolymers were investigated in this study. Also, the biodegradable behavior of CE diblock copolymer was investigated in vitro.

2. Materials and methods

2.1. Materials

Methoxy PEG (MW = 5000) (MPEG), dialysis tube (molecular weight cut-off (MWCO) = 2000, 12,000), all-*trans*-retinoic acid, and 3-(4,5-dimethylthiazol-2-yl)-2,5-diphenyl tetrazolium bromide (MTT) were purchased from Sigma, USA. ε-Caprolactone, acetone, methanol, dimethylformamide (DMF), dichloromethane (DCM), diethyl ether, and tetrahydrofuran (THF) were purchased from Aldrich Chem., USA. α-Minimum essential medium (α-MEM) was purchased from GIBCO (Invitrogen, USA). All other chemicals and reagents were used as extra reagent grade in all of the experiments.

2.2. Synthesis of PCL/PEG diblock copolymer

CE diblock copolymers were synthesized by a non-catalyzed ring-opening polymerization of ε-caprolactone in the presence of MPEG as shown in Fig. 1

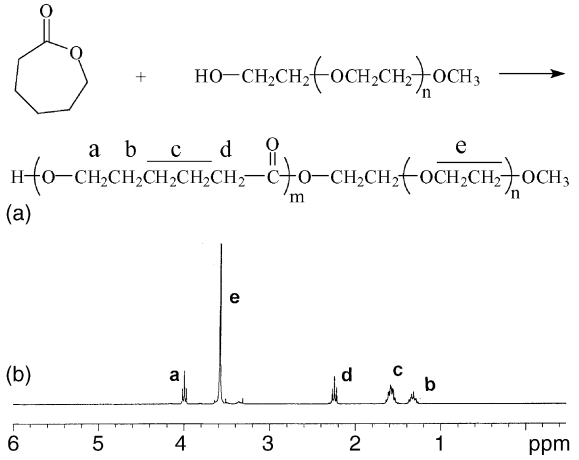

Fig. 1. Synthesis scheme of CE diblock copolymer and typical ^{1}H NMR spectra.

(Cerrai et al., 1989). MPEG and ε-caprolactone were mixed in a round-bottomed flask under vacuum. The mixture was cooled and degassed with pump. The round-bottomed flask was sealed off and placed in an oil bath at 180 °C. After the polymerization was completed, the resulting product was cooled at room temperature and then dissolved in DCM. The solution was precipitated into an excess amount of cold ethanol and filtered to remove the unreacted MPEG homopolymer and ε-caprolactone monomers. The precipitates were washed with diethylether three times and then dried in a vacuum oven for 3 days.

2.3. Measurement of fluorescence spectroscopy

To measure the critical association concentration (CAC) of CE diblock copolymer using fluorescence spectroscopy, CE diblock copolymer solutions without drug were prepared as follows: 40 mg of CE block copolymer were dissolved in 4 ml of acetone and dropped into 10 ml of deionized water under reduced pressure. Residual solvent was removed using rotary evaporator and then dialyzed using molecular cut-off 2000 g/mol dialysis tube (Sigma Chem., USA) against 1 l × 3 of distilled water for 3 h and then 3–4 h during 2 days. Resultant solution was adjusted to the various concentrations of block copolymers.

CAC of the CE diblock copolymers was estimated to prove the potential of micellar structure formation under aqueous environment by the measurement of fluorescence spectroscopy (Shimadzu F-7000 spectrofluorometer, Shimadzu, Tokyo, Japan) using pyrene as a probe (Wilhelm et al., 1991; Kwon et al., 1993). To get sample solutions, a known amount of pyrene in acetone was added to each of a series of 20 ml vials and the acetone evaporated. The amount was adjusted to give a pyrene concentration in the final solution of either 6.0×10^{-7} M. The 10 ml of various solutions were added to each vial and then heated for 3 h at 65 °C to equilibrate the pyrene and the micelles and leaved to cool overnight at room temperature. Emission wavelength was 390 nm for excitation spectra. Excitation and emission bandwidths were 1.5 and 1.5 nm, respectively.

2.4. Preparation of core-shell type nanoparticles containing atRA

CE diblock copolymer nanoparticles containing atRA prepared by nanoprecipitation technique was as follows: CE diblock copolymer and atRA dissolved in 4 ml of acetone or THF were poured into 10 ml of deionized water. Solvent was evaporated using rotary evaporator. Resulting solution was centrifuged at 40,000 rpm for 20 min (4 °C). Harvested nanoparticles were washed with deionized water. After that, resulting solution was used for analysis or lyophilization.

CE diblock copolymer nanoparticles containing atRA prepared by dialysis technique was as follows: CE diblock copolymer and atRA dissolved in 4 ml DMF were introduced into dialysis tube (MWCO 2000) and then the solution was dialyzed against 1 l × 6 of deionized water for 12 h following 1 l × 3 water for additional 12 h. After that, resulting solution was used for analysis or lyophilization. All procedures for preparation were carried out at darkened condition to avoid drug degradation by light.

To measure drug contents and loading efficiency, 5 mg of lyophilized nanoparticles were dissolved in acetone and drug concentration was measured at 365 nm with UV spectrophotometer (UV-1200, Shimadzu, Japan). The 5 mg of empty nanoparticles were dissolved in acetone for blank test to verify interference of CE diblock copolymer:

$$\text{Drug contents} = \frac{\text{amount of atRA in the nanoparticles}}{\text{weight of nanoparticles}} \times 100$$

$$\text{Loading efficiency} = \frac{\text{residual amount of atRA in the nanoparticles}}{\text{feeding amount of atRA}} \times 100$$

2.5. ^{1}H nuclear magnetic resonance (NMR) spectrometer measurement

In order to estimate the copolymer compositions and the molecular weights of the PCL blocks, the ^{1}H NMR spectra of the copolymers were measured in $CDCl_3$ using a 300 MHz NMR spectrometer (FT-NMR, Bruker AC-300F, 300 MHz). As the number-average molecular weight of PEG (5000) is known, one can estimate the number-average molecular weights of the PCL block and the copolymer composition as calculated from the peak intensities in the spectrum assigned to both polymers.

To approve the core-shell type structure and drug loading characteristics of CE block copolymer, ^{1}H NMR spectra were registered in $CDCl_3$ and D_2O. The concentration of the polymeric core-shell type nanoparticles was 1.0 wt.% in $CDCl_3$ and 0.5 wt.% in D_2O.

2.6. Measurement of particle size

Size of nanoparticles was measured with a photon correlation spectroscopy (Zetasizer 3000, Malvern instruments, England) with an He–Ne laser beam at a wavelength of 633 nm at 25 °C (scattering angle of 90°). A nanoparticle solution prepared by dialysis method was used for particle size measurement (concentration: 0.1 wt.%) and measured without filtering.

2.7. Drug release studies

Drug contents in nanoparticles are determined as follows: atRA-encapsulated nanoparticles were prepared as described above (in Section 2.4) and final aqueous solution adjusted to 20 ml (i.e. 40 mg of polymer per 20 ml of water). The 2 ml of adjusted solution was introduced into dialysis tube (MW cut-off 12,000) and dialysis tube introduced into a bottle with 198 ml of phosphate buffered saline (PBS, 0.1 M, pH 7.4). Release test was performed at 37 °C with stirring rate of 50 rpm. The whole release medium was exchanged with fresh medium at predetermined time to maintain the sink condition. Released amount of drug was measured at 365 nm with UV spectrophotometer (UV-1200, Shimadzu, Japan).

2.8. In vitro degradation test of CE block copolymer nanoparticles

In order to study the degradation behavior of CE core-shell type nanoparticles, the dialyzed nanoparticle solution was incubated in PBS (0.1 M, pH 7.4). The 100 mg of CE diblock copolymer were dissolved in 10 ml of acetone. The solution was dropped into 25 ml of water with gentle magnetic stirring followed by dialysis using a molecular cut-off 2000 g/mol dialysis tube for 1 day against 3 l of deionized water and then PBS (0.1 M, pH 7.4) for 6 h. The dialyzed aqueous solution was adjusted to 50 ml with PBS solution and each 10 ml (i.e., 10 ml of aqueous solution containing 20 mg of CE diblock copolymer) were subsequently introduced into the dialysis tube (molecular weight cut-off 2000 g/mol). The dialysis tubes were then introduced into a bottle with 10 ml PBS and incubated at 50 rpm in 37 °C. The medium was exchanged with fresh PBS everyday. At specific time intervals, dialyzed polymer solution in the dialysis tube was taken and dialyzed against distilled water for 6 h to remove trace elements of phosphate. The resultant solution was freeze-dried for the analysis of molecular weight changes of the PCL block by ^{1}H NMR as described above.

2.9. Cell culture study

Brain tumor cell line, U87MG, U251MG, and U343MG-A, were obtained from American Type Culture Collection (ATCC, USA). Cells were maintained at α-MEM containing 10% fetal bovine serum in a CO_2 incubator (5% CO_2 at 37 °C).

The effect of atRA-encapsulated CE nanoparticles on cell growth is determined using a MTT cell proliferation assay. Nanoparticles containing atRA was diluted further using PBS. U251MG, malignant glioma cell line, was seeded at a density of 5×10^3 per well in 96-well plates with α-MEM containing 10% fetal bovine serum and incubated overnight in a CO_2 incubator (5% CO_2 at 37 °C). After that, PBS containing atRA-encapsulated nanoparticles is added. After 2-day incubation, the cell viability assay is performed.

The relationship between drug concentration and tumor cell-killing was determined using the reduction of MTT colorimetric assay originally described by Mosman and modified by Alley et al. (1988) and Sladowski et al. (1993). After the incubation period, tumor cells were exposed to 30 μl of MTT (5 mg/ml) for 4 h. Formazan crystals were then solubilized with DMSO or acid/alcohol, with absorbance (570 nm test/630 nm reference) determined using an automated computer-linked microplate reader (Molecular Device, USA). Each concentration of drugs was studied in triplicate. The amount of formazan present is proportional to the number of viable cells, as only living cells will reduce MTT to blue formazan. Results were expressed as a percentage of the absorbance present in drug-treated cells compared to that in the control cells.

3. Results and discussion

3.1. Characterization of CE diblock copolymer and its core-shell type nanoparticles

CE diblock copolymers were synthesized by ring-opening polymerization of ε-caprolactone monomer in the presence of MPEG without catalysts. An active hydrogen atom at one end of MPEG chains acts as an initiator and induces a selective acyl-oxygen cleavage of ε-caprolactone (Fig. 1). Since PCL homopolymer is a semicrystalline polymer and has hydrophobic characteristics contributing to a long degradation time in vivo, copolymerization with MPEG should be changed the degradation period and physicochemical properties.

CE diblock copolymers with different molecular weights were prepared by changing the molar ratio of MPEG/ε-caprolactone monomer. Their MW and composition were calculated from ^{1}H NMR spectra. The unit ratio of MPEG and ε-caprolactone was obtained from peak intensities of the methylene proton of MPEG chain (3.7 ppm) and methylene proton (4.13 ppm) in ε-caprolactone units (Fig. 1(b)). Calculated results were summarized in Table 1.

CE diblock copolymer would have potential to form core-shell type nanoparticles and associate at critical concentration since it has amphiphilic characteristics in the aqueous environment. The formation of core-shell type structures was confirmed by a fluorescence probe technique using pyrene as a hydrophobic probe at various concentrations as shown in Fig. 2. Pyrene will be preferentially partitioned into hydrophobic environment with a concurrent change of the photophysical properties of the molecules (Wilhelm et al., 1991; Kwon et al., 1993). Wilhelm et al. (1991) reported micelle formation of polystyrene (PS) and PEO di- or tri-block copolymers in water using a fluorescence technique with pyrene as a hydrophobic probe and determined the critical micelle concentration from the fluorescence and excitation spectra, as pyrene partitions between aqueous and micellar environments.

Table 1
Characterization of CE diblock copolymers and corresponding core-shell type nanoparticles

	M_n of PCL	Total M_n	Particle size (nm)	CAC (g/l)
CE-1	1270	6270	71 ± 21	0.0151
CE-2	3200	8200	82 ± 14	0.0032
CE-3	4250	9250	93 ± 31	0.0025

M_n: number-average molecular weight; CAC: critical association concentration.

Fig. 2 shows fluorescence spectra of pyrene at a fixed excitation wavelength of 339 nm were observed in the presence of varying concentrations of CE diblock copolymer. The higher the concentration of CE diblock copolymer, the higher the fluorescence intensity, which indicates the formation of self-assembling nanoparticles in water. Pyrene will preferentially partition into hydrophobic microdomains with a concurrent change in the molecules photophysical properties. Total fluorescence intensity of a fluorescence probe increases on self-association of CE block copolymer. Changes of total fluorescence intensity were negligible at the low concentrations of CE block copolymer. As the concentration of CE diblock copolymer increased, the total fluorescence intensity increased logarithmically at a critical concentration of CE.

Fig. 3 shows fluorescence excitation spectra of pyrene (6.0×10^{-7} M) in the presence of CE block copolymer at various concentrations. In the excitation spectrum, a red shift was observed with increasing concentration of CE block copolymer. A red shift of pyrene in the excitation spectrum was observed in the study of micelle formation of PS–PEO block copolymers (Wilhelm et al., 1991). The (0, 0) bands

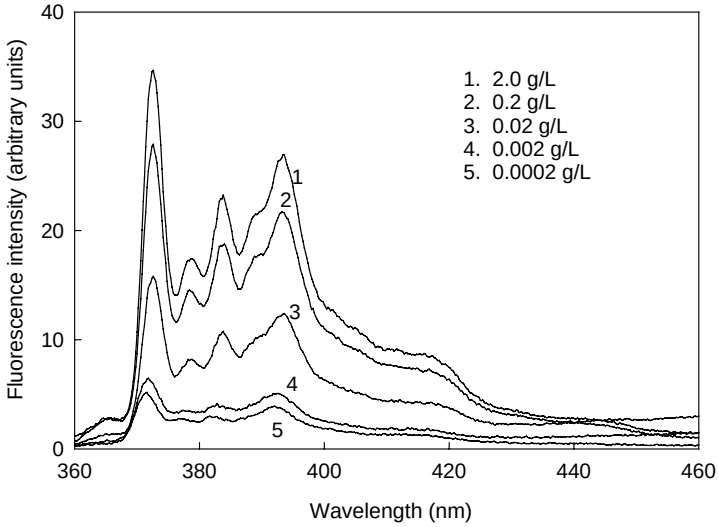

Fig. 2. Fluorescence spectra of pyrene/CE-2 against concentration of CE-2 in distilled water (excitation wavelength: 339 nm).

in the pyrene excitation spectra were examined and compared with the intensity ratio $I_{337.2}/I_{334}$. This ratio takes the value characteristic of pyrene, in water at low concentrations and the value of pyrene, entirely in the hydrophobic domain. A plot of $I_{337.2}/I_{334}$ versus $\log c$ is shown in Fig. 3(b). A flat region in the low concentration and sigmoidal region in the crossover region was noted and CAC value of 0.0032 g/l was obtained. As shown in Table 1, the higher the MW of polymer the lower the CAC.

3.2. Characterization of atRA-entrapped core-shell type nanoparticles of CE diblock copolymers

Drug loading characteristics were studied under various experimental conditions. As shown in Table 2, drug contents and loading efficiency increased with increase in the MW of PCL block of CE. Since larger PCL block length will result in more hydrophobic polymer, the larger the PCL block the higher the hydrophobic interaction with drugs. Also, particle size increased at larger PCL block length. When initial drug concentration increased, the drug contents and particle size increased. With the increase in polymer concentration at the initial stage of nanoparticle preparation, there was a decrease in the particle size as well as the loading efficiency. Solvent used and preparation method also affected drug contents and loading efficiency. When DMF was used to make nanoparticles by dialysis method, drug contents and loading efficiency decreased whereas no difference was detected with THF. These results showed that

Table 2
Drug loading characteristics and particle size of core-shell type nanoparticles of CE diblock copolymers

Polymer (mg)	atRA (mg)/solvent	Drug contents (%, w/w)	Loading efficiency (%, w/w)	Particle size (nm)
CE-1 (40)	2/acetone	3.3	68.3	279 ± 72
CE-2 (40)	2/acetone	3.8	79.7	284 ± 98
CE-3 (40)	2/acetone	4.3	93.1	336 ± 106
CE-3 (40)	5/acetone	10.8	97.3	390 ± 175
CE-3 (80)	2/acetone	2.2	91.8	313 ± 103
CE-3 (40)	2/THF	4.1	85.1	458 ± 178
CE-3 (40)	2/DMF	3.7	76.4	276 ± 81

CE: poly(ϵ-caprolactone)/poly(ethylene glycol) diblock copolymer; atRA: all-*trans*-retinoic acid; THF: tetrahydrofuran; DMF: dimethylformamide.

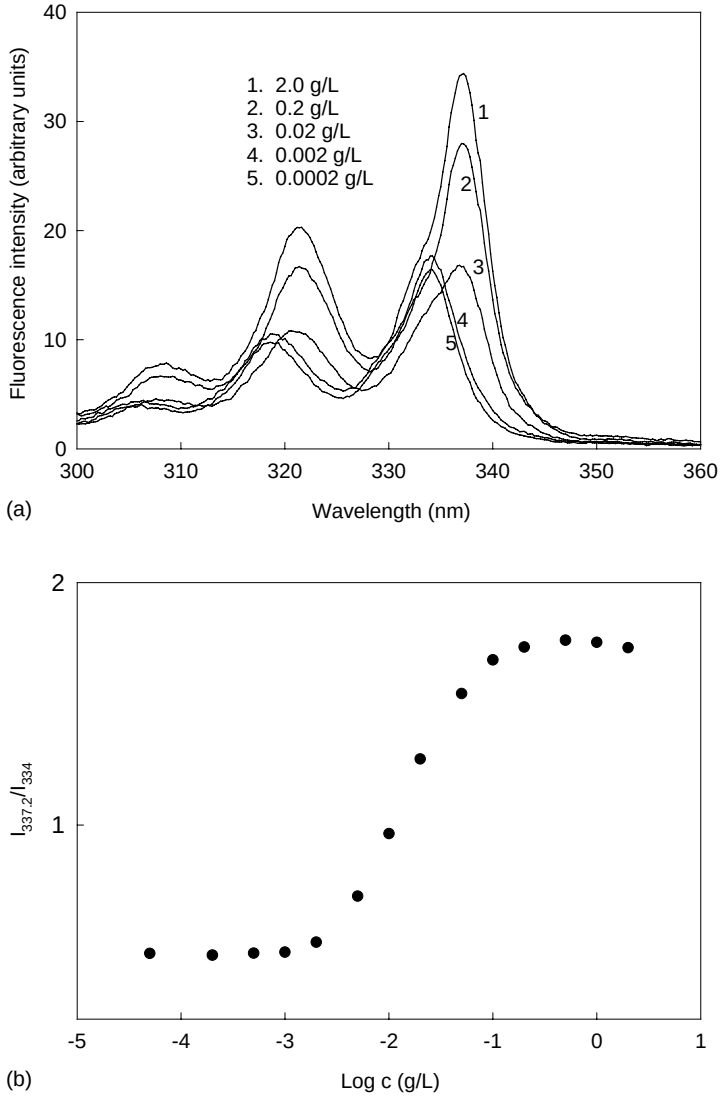

Fig. 3. Fluorescence excitation spectra of pyrene/CE-2 against concentration of CE-2 in distilled water (emission wavelength: 390.0 nm) (a) and plots of the intensity ratio of $I_{337.2}/I_{334}$ from pyrene excitation spectra vs. $\log c$ for block copolymer against concentration of CE in distilled water (b).

drug loading characteristics were affected by various formulation factors.

Further evidence of core-shell type nanoparticles of CE-3 block copolymer and, limited mobility of the PCL chain and drug loading in the core of the nanoparticles were obtained with ^{1}H NMR in $CDCl_3$ and D_2O as shown in Fig. 4. Since both of the PCL and PEG blocks are easily dissolved in $CDCl_3$ (Fig. 4(b)), the core-shell structure was not expected. In $CDCl_3$, the characteristic peak of the methyl protons of the PCL segment was shown to be about 1.4, 1.65, 2.3 and 4.13 ppm, respectively. Also, in that solvent, protons of the ethylene glycol of the PEG segment was shown in 3.6–3.7 ppm. But, in D_2O, characteristic peaks of the PCL blocks completely disappeared, whereas peculiar peaks of the PEG block remained as shown in Fig. 4(d). These results indicated that protons of PCL block display restricted motions within the inner-core

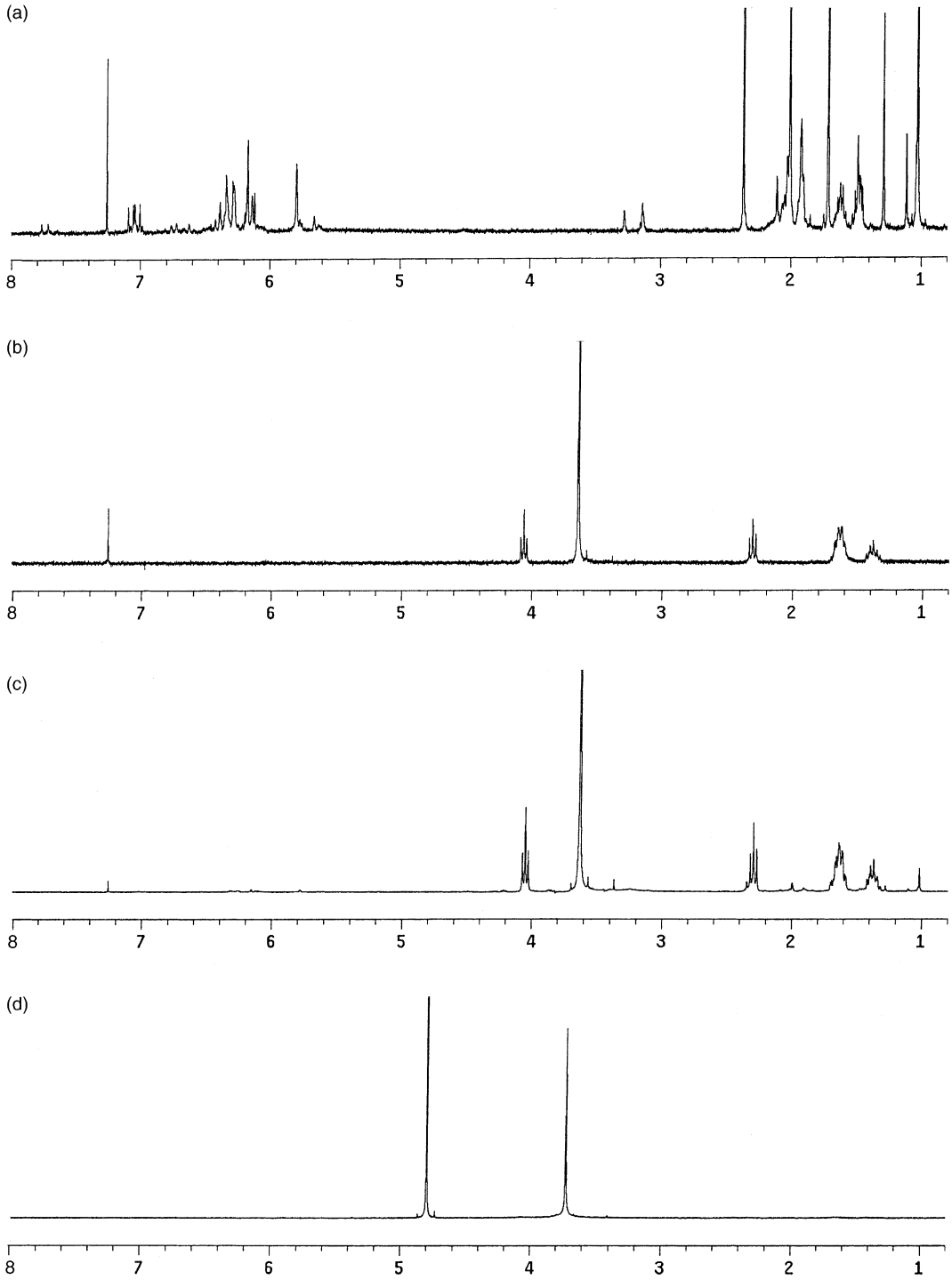

Fig. 4. ^{1}H NMR spectra of CE-3 core-shell type nanoparticles. atRA (a), CE-3 empty nanoparticles (b), and atRA-entrapped CE-3 nanoparticles dissolved in $CDCl_3$ (c) and redistributed in D_2O (d).

and PCL block has a rigid solid structure, whereas PEG blocks are existed as a liquid state in the aqueous environment. Kwon et al. (1993) also reported that poly(β-benzyl-L-aspartate) (PBLA)/PEO diblock copolymer has a rigid PBLA core. In their results, the peaks of 7.4 and 5.2 ppm did not completely disappear and this result suggested that PBLA/PEO diblock copolymer micelles may have a relatively less rigid core compared to CE core-shell type nanoparticles. Also, drug entrapment into inner-core of the core-shell type nanoparticles was approved with ^{1}H NMR in $CDCl_3$ and D_2O. The characteristic peaks of drug itself (Fig. 4(a)) disappeared in D_2O (Fig. 4(d)), whereas peaks of PEG remained. But, in $CDCl_3$, both characteristic peaks of CE diblock copolymer and drug appeared as shown in Fig. 4(c). These results clearly showed that hydrophobic drugs were successively entrapped into inner-core of the core-shell type nanoparticles with hydrated outershell of PEG.

X-ray powder diffraction spectra were registered to investigate the physicochemical characteristics of atRA-entrapped CE-3 core-shell type nanoparticles. Fig. 5 shows the X-ray powdered diffraction (XRD) scans of atRA-entrapped CE-3 core-shell type nanoparticles. XRD patterns showed typical sharp peaks in atRA drug crystals (Fig. 5(a)) while empty nanoparticles of CE-3 nanoparticles showed relatively simple peaks. When atRA-entrapped into CE-3 nanoparticles, the specific drug crystal peaks were not observed in the XRD patterns (Fig. 5(c)). It was thought that drug crystallites exhibited sharp specific crystal peaks when existing as drug crystals but drug existed as molecular dispersion inside the nanoparticles after entrapped into it (Gref et al., 1994; Jeong et al., 1998, 2002). On the other hand, small crystal peaks of drug were observed at the high drug entrapment (Fig. 5(d)). These results might be due to that the drug was aggregated inside the nanoparticles and drug crystals formed in the core of the nanoparticles. Also, drugs can be retained on the surface of the nanoparticles.

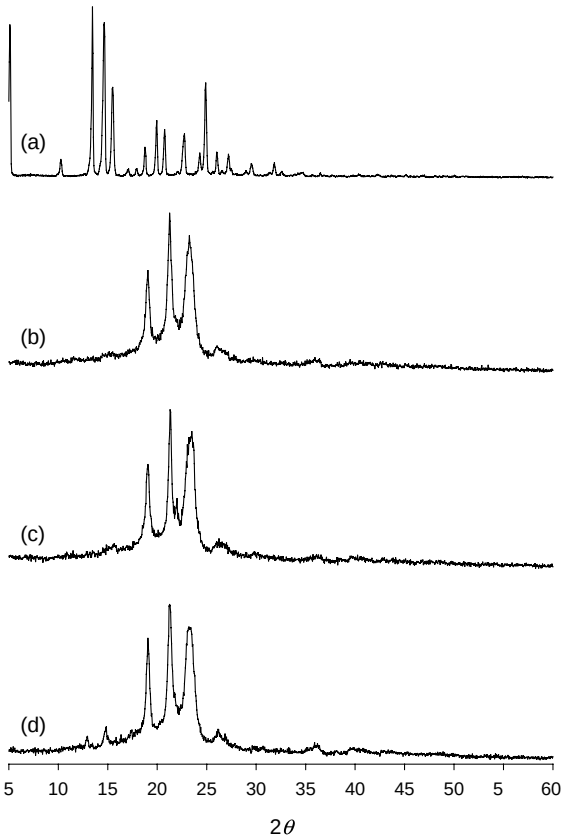

Fig. 5. X-ray powder diffraction patterns of CE-3 core-shell type nanoparticles. atRA (a), CE-3 empty nanoparticles (b), atRA-entrapped CE-3 nanoparticles (drug contents: 4.26 wt.%) (c) and atRA-entrapped CE-3 nanoparticles (drug contents: 10.84 wt.%) (d).

3.3. Drug release characteristics from core-shell type nanoparticles of CE diblock copolymer

atRA release characteristics from core-shell type nanoparticles of CE diblock copolymer are shown in Fig. 6. As shown in Fig. 6(a), atRA release was faster from CE-2 nanoparticles than from CE-3 nanoparticles. Since CE-3 is more hydrophobic than CE-2, less hydrophobic environment at CE-2 might result in faster release kinetics of hydrophobic drug, atRA. Also, differences of drug contents between CE-2 and CE-3 nanoparticles might be another reason for difference in release characteristics. atRA was continually released in vitro over 15 days and the release pattern showed almost pseudo-zero-order kinetics. Fig. 6(b) shows the effect of drug contents on the release of atRA. As shown in Fig. 6(b), the higher the drug contents, the slower the drug release kinetics. Several authors reported the same phenomena (Gref et al., 1994; Jeong et al., 1998; Kwon et al., 1995). Gref et al. (1994) reported that crystallization of hydrophobic

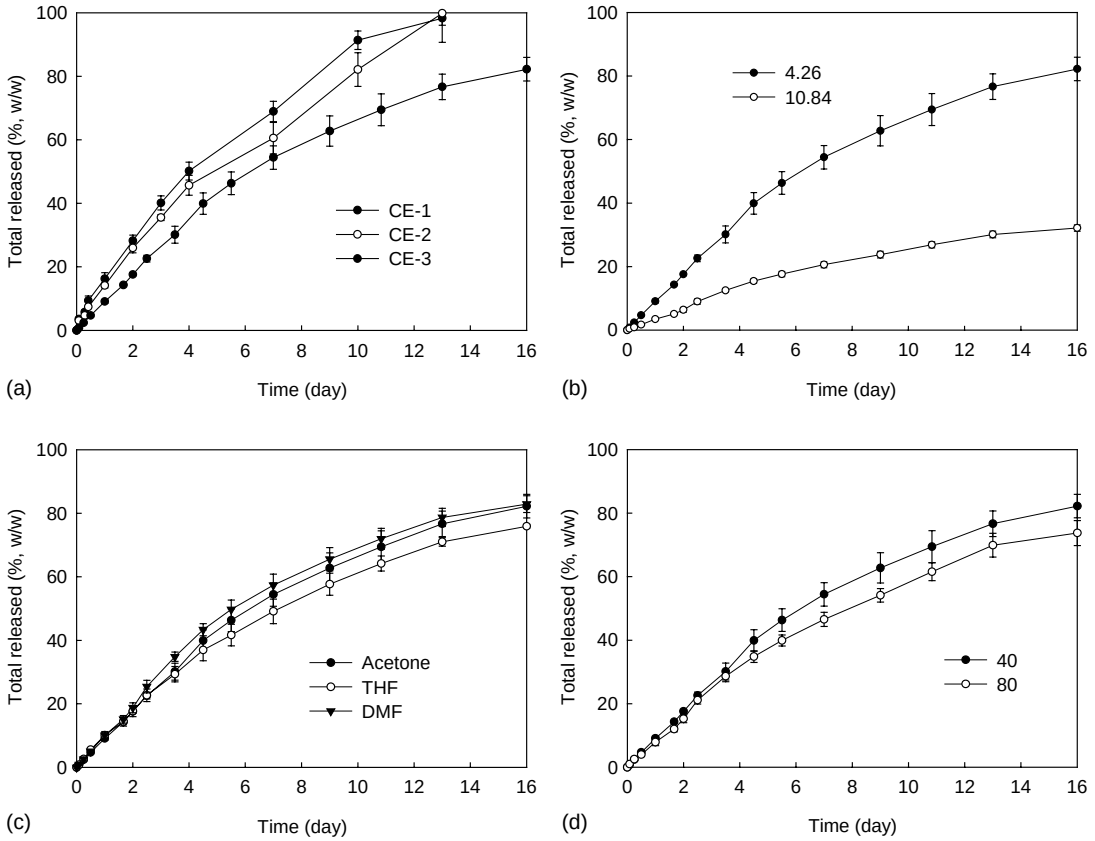

Fig. 6. atRA release from core-shell type nanoparticles of CE diblock copolymers. The effect of MW of diblock copolymer (a), drug contents (b), solvent used (c), and polymer concentration (d) on the drug release kinetics. CE-3 were used at (b)–(d).

drug occurred inside the nanoparticles and, especially, at higher drug loading contents, a phase separation occurs, leading to the crystallization of part of the drug in the nanoparticles. Then, hydrophobic drugs loaded into nanoparticles are released more slowly at higher drug loading contents in contrast to hydrophilic water-soluble drugs. Also, our group observed that atRA release kinetics from the nanoparticles with higher drug loading contents has slower release kinetics from than nanoparticles with lower drug-loading contents. On the other hand, at low drug loading, atRA might be relatively present as a molecular dispersion inside the nanoparticles (Gref et al., 1994). The crystallized drug should dissolve and diffuse more slowly into the outer aqueous phase than in that of molecular dispersion. These characteristics of drug release were

Table 3
Degradation characteristics of core-shell type nanoparticles of CE diblock copolymer during 10 days

	Initial M_n of PCL	Initial total M_n	Residual MW of PCL	Residual total MW	Degradation ratio[a]
CE-1	1270	6270	1200	6200	5.5
CE-2	3200	8200	3070	8070	4.1
CE-3	4250	9250	4080	9080	4.0

PCL: poly(ϵ-caprolactone); M_n: number-average molecular weight; MW: molecular weight.
[a] Degradation ratio = [(initial MW of PCL − PCL MW at time T)/initial MW of PCL] × 100.

supported by XRD results as already shown in Fig. 5. Fig. 6(c) shows the effect of solvent used and preparation method on the drug release kinetics. As shown in Fig. 6(c), nanoparticles prepared by various solvent were not significantly changed in their drug release. Nanoparticles prepared using THF showed slower release rate compared to nanoparticles by acetone although drug contents of nanoparticles by THF were lower than those of acetone. It was suggested that nanoparticles by THF were larger than those of acetone, and larger nanoparticles may induce slower drug release rate than small nanoparticles. Fig. 6(d) shows the effect of polymer concentration on the drug release kinetics. Drug release from higher polymer concentration was slower than lower polymer concentration although drug release was not significantly different.

To study the drug release mechanism from core-shell type nanoparticles of CE diblock copolymer, degradation tests of core-shell type nanoparticles were performed in vitro. To observe the degradation behavior of core-shell type nanoparticles of CE diblock copolymer, nanoparticles were incubated in the PBS and the number-average molecular weight (M_n) was analyzed by ^{1}H NMR spectroscopy. Since PEG block is not degradable in physiological solution during degradation of PCL blocks, MW of PEG is constantly same to initial MW during degradation test. The residual PCL block can expect continuous degradation and residual PCL block could be calculated by ^{1}H NMR spectroscopy and their results were summarized in Table 3. As shown in Table 3, both core-shell type nanoparticles of CE diblock copolymer were degraded very slowly, i.e. only 4.1% of CE-2 and 4.0% of CE-3 were degraded during 10 days. These results indicated that release kinetics of atRA from core-shell type nanoparticles were dominantly controlled by diffusion rather than degradation mechanism.

3.4. Cell cytotoxicity

To investigate efficacy of atRA-entrapped nanoparticles compared to atRA itself, cell cytotoxicity using U251MG and U343MG cell lines were performed by MTT test. To test cell cytotoxicity, atRA-entrapped CE-3 nanoparticles were filtered and diluted with α-MEM and PBS to adjust the drug concentration. Fig. 7(a)–(c) shows the cytotoxicity of atRA and atRA-entrapped nanoparticles against U251MG, U343MG, and U87MG cells, respectively. As shown in Fig. 7(a) and (b), atRA-entrapped nanoparticles showed enhanced cytotoxicity below 10 μg of at RA and almost similar or lower cytotoxicity at the 50 μg of atRA at both of the cell lines while similar cytotoxicity was obtained with U87MG cells at all concentration range. These results might be due to that, when it

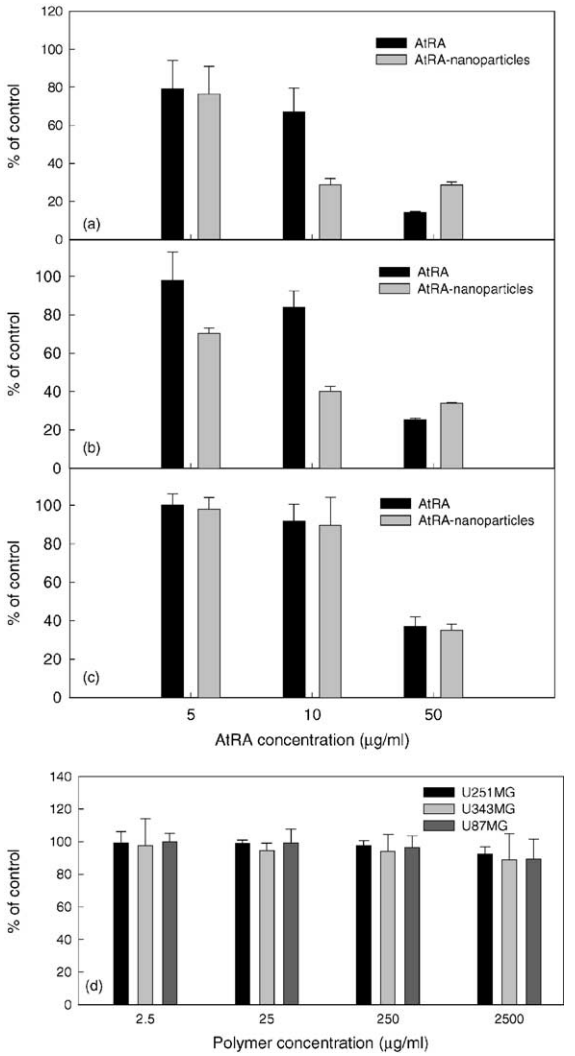

Fig. 7. Cell growth inhibition of U251MG, U343MG, and U87MG cell lines by atRA-entrapped nanoparticles after 2 days. atRA and atRA-entrapped nanoparticles of CE-3 against U251MG (a), U343MG (b), and U87MG (c); empty nanoparticles against U251MG, U343MG, and U87MG (d). The value was mean of eight wells and expressed as S.D.

encapsulated into nanoparticles, atRA was relatively stable against stress such as temperature, light, etc., resulting efficacy of atRA could be maintained easily inside the nanoparticles. Also, these results showed that atRA does not lose its efficacy during nanoencapsulation process. Fig. 7(d) showed that cytotoxicity of empty nanoparticles against U251MG, U343MG, and U87MG cell lines. These results showed CE block copolymer nanoparticles does not affect significantly on the cytotoxicity of atRA-encapsulated nanoparticles.

4. Conclusion

In this study CE diblock copolymers were synthesized to make core-shell type nanoparticles and entrapment of atRA into the nanoparticles. CAC value for the association behavior of CE diblock copolymer in water were evaluated using fluorescence spectroscopy. The higher the MW of CE diblock copolymer the lower the CAC. Drug contents and loading efficiency increased according to the increase in MW of PCL block of CE and polymer concentration. Solvent used and preparation method also affected drug contents and loading efficiency. Limited mobility of the PCL chain and drug loading in the core of the nanoparticles were obtained in the results of ^{1}H NMR using $CDCl_3$ and D_2O. The specific peaks of PCL block of copolymer and drug appeared in $CDCl_3$, disappeared at D_2O, indicating hydrophobic core and hydrophilic outershell were formed in water. XRD results also indicated that hydrophobic drug was entrapped into the core of nanoparticles. atRA release was faster at smaller MW of copolymer and lower drug contents. Nanoparticles prepared by DMF resulted in the fastest release rates whereas those of THF resulted in the slowest release rate. Release kinetics of atRA were predominantly controlled by diffusion rather than degradation mechanism. Cytotoxicity of atRA against U251MG, U343MG-A, and U87MG cell lines increased by nanoencapsulation while empty nanoparticles of CE diblock copolymer was not significantly affected.

Acknowledgements

The study was supported financially by Chonnam National University in the program (2002).

References

Achkar, C.C., Bentel, J.M., Boylan, J.F., Scher, H.I., Gudas, L.J., Miller, W.H., 1994. Differences in the pharmacokinetic properties of orally administered all-*trans*-retinoic acid and 9-*cis*-retinoic acid in the plasma of nude mice. Drug Metab. Disp. 22, 451–458.

Alley, M.C., Scudiero, D.A., Monks, A., 1988. Feasibility of drug screening with panels of human tumor cell lines using a microculture tetrazolium assay. Cancer Res. 48, 589–601.

Bouterfa, H., Picht, T., Keb, D., Herbold Mc, S.C., Noll, E., Black, P.M., Roosen, K., Tonn, J.C., 2000. Retinoids inhibit human glioma cell proliferation and migration in primary cell cultures but not in established cell lines. Neurosurgery 46, 419–430.

Cerrai, P., Tricoli, M., Andruzzi, F., Paci, M., 1989. Polyether–polyester block copolymer by non-catalyzed polymerization of ε-caprolactone with poly(ethylene glycol). Polymer 30, 338–343.

Defer, G.L., Adle-Biassette, H., Ricolfi, F., Martin, L., Authier, F.J., Chomienne, C., Degos, L., Degos, J.D., 1997. All-*trans* retinoic acid in relapsing malignant gliomas: clinical and radiological stabilization associated with the appearance of intratumoral calcifications. J. Neurooncol. 34, 169–177.

Estey, E., Thall, P.F., Mehta, K., Rosenblum, M., Brewer Jr., T., Simmons, V., Cabanillas, F., Kurzrock, R., Lopez-Berestein, G., 1996. Alterations in tretinoin pharmacokinetics following administration of liposomal all-*trans* retinoic acid. Blood 87, 3650–3654.

Giannini, F., Maestro, R., Vukosa, T., Vljevic, T., Pomponi, F., Boiocchi, M., 1997. All-*trans*, 13-*cis* and 9-*cis* retinoic acids induce a fully reversible growth inhibition in HNSCC cell lines: implications for in vivo retinoic acid use. Int. J. Cancer 70, 194–200.

Gref, R., Minamitake, Y., Peracchia, M.T., Trubetskoy, V., Torchilin, V., Langer, R., 1994. Biodegradable long-circulating polymeric nanospheres. Science 263, 1600–1603.

Huang, E.J., Ye, Y.C., Chen, S.R., Chai, J.R., Lu, J.X., Zhoa, L., Gu, L.J., Wang, Z.Y., 1988. Use of all-*trans*-retinoic acid in the treatment of acute promyelocytic leukemia. Blood 72, 567–572.

Jeong, Y.I., Cheon, J.B., Kim, S.H., Nah, J.W., Lee, Y.M., Sung, Y.K., Akaike, T., Cho, C.S., 1998. Clonazepam release from core-shell type nanoparticles in vitro. J. Contr. Release 51, 169–178.

Jeong, Y.I., Shim, Y.H., Song, K.C., Park, Y.G., Ryu, H.W., Nah, J.W., 2002. Testosterone-encapsulated surfactant-free nanoparticles of poly(DL-lactide-co-glycolide): preparation and release behavior. Bull. Korean Chem. Soc. 23, 1579–1584.

Kalmekerian, G.P., Jasti, R.K., Celano, P., Nelkin, B.D., Marby, M., 1994. All-*trans*-retinoic acid alters myc gene expression and inhibits in vitro progression in small-cell lung cancer. Cell Growth Differ. 5, 55–60.

Krupitza, G., Hulla, W., Harant, H., Dittrich, E., Kallay, E., Huber, H., 1995. Retinoic acid induced death of ovarian carcinoma cells correlates with c-myc stimulation. Int. J. Cancer 61, 649–657.

Kwon, G., Naito, M., Yokoyama, M., Okano, T., Sakurai, Y., Kataoka, K., 1993. Micelles based on AB block copolymers of poly(ethylene oxide) and poly(β-benzyl-L-aspartate). Langmuir 9, 945–949.

Kwon, G.S., Naito, M., Yokoyama, M., Okano, T., Sakurai, Y., Kataoka, K., 1995. Physical entrapment of adriamycin in AB block copolymer micelles. Pharm. Res. 12, 192–195.

La, S.B., Okano, T., Kataoka, K., 1996. Preparation and characterization of the micelle-forming polymeric drug indomethacin-incorporated poly(ethylene oxide)–poly(β-benzyl-L-aspartate) block copolymer micelles. J. Pharm. Sci. 85, 85–90.

Le Doze, F., Debruyne, D., Albessard, F., Barre, L., Defer, G.L., 2000. Pharmacokinetics of all-*trans* retinoic acid, 13-*cis* retinoic acid, and fenretinide in plasma and brain of rat. Drug Metab. Dispos. 28, 205–208.

Lee, J.H., Kopecek, J., Andrade, J.D., 1989. Protein-resistant surfaces prepared by PEO-containing block copolymer surfactants. J. Biomed. Mater. Res. 23, 351–368.

Lin, H.S., Chean, C.S., Ng, Y.Y., Chan, S.Y., Ho, P.C., 2000. 2-Hydroxypropyl-β-cyclodextrin increases aqueous solubility and photostability of all-*trans*-retinoic acid. J. Clin. Pharm. Ther. 25, 265–269.

Morris-Kay, G. (Ed.), 1992. Retinoids in Normal Development and Teratogenesis. Oxford Science Publications, Oxford.

Muindi, J.R.F., Frankel, S.R., Miller, W.H., Jakubowski, A., Scheinberg, D.A., Young, C.W., Dmitrovsky, E., Warrell, R.P., 1992. Continuous treatment with all-*trans*-retinoic acid causes a progressive reduction in plasma drug concentrations: implications for relapse and retinoid "resistance" in patients with acute promyelocytic leukemia. Blood 79, 299–303.

Noll, E., Miller, R.H., 1994. Regulation of oligodendrocyte differentiation: a role for retinoic acid in the spinal cord. Development 120, 649–660.

Rotan, R., 1991. Retinoids as modulators of tumor cell invasion and metastasis. Semin. Cancer Biol. 2, 197–208.

Sladowski, D., Steer, S.J., Clothier, R.H., Balls, M., 1993. An improved MTT assay. J. Immunol. Meth. 157, 203–207.

Szuts, E.Z., Harosi, F.I., 1991. Solubility of retinoids in water. Arch. Biochem. Biophys. 287, 297–304.

Wilhelm, M., Zhao, C.L., Wang, Y., Xu, R., Winnik, M.A., Mura, J.L., Riess, G., Croucher, M.D., 1991. Poly(styrene-ethylene oxide) block copolymer micelle formation in water: a fluorescence probe study. Macromolecules 24, 1033–1040.

Yokoyama, M., Miyauchi, M., Yamada, N., Okano, T., Sakurai, Y., Kataoka, K., 1990. Characterization and anticancer activity of the micelle-forming polymeric anticancer drug adriamycin-conjugated poly(ethylene glycol)–poly(aspartic acid) block copolymer. Cancer Res. 50, 1693–1700.